

8. DATA REPORT: PALEOMAGNETISM OF BASALTIC ROCKS CORED FROM WESTERN PACIFIC DSDP AND ODP BOREHOLES¹

William W. Sager²

INTRODUCTION

Oceanic basalts and other related igneous rocks are considered excellent recorders of the Earth's paleomagnetic field. Consequently, basalt core paleomagnetic data are valuable for the constraints they provide on plate tectonic motions, especially for oceanic plates such as the Pacific. Unfortunately, few Deep Sea Drilling Project (DSDP) and Ocean Drilling Program (ODP) boreholes have been cored very deeply into the ocean crust. The result is that there are only a few sites at which a large enough number of basalt flows have been cored to properly average secular variation (e.g., Kono, 1980; Cox and Gordon, 1984). Furthermore, there are a number of sites where basaltic core samples were retrieved but the cores were not measured. Often this occurs because leg scientists had more important sections to work on, or the section was ignored because it was too short to record enough time to average secular variation and obtain a reliable paleolatitude. Even though it may not be possible to determine a precise paleolatitude from such short sections, measurements from a small number of flows are important because they can be combined with other coeval paleomagnetic data from the same plate to calculate a paleomagnetic pole (Gordon and Cox, 1980; Cox and Gordon, 1984). For this reason, I obtained samples for paleomagnetic measurements from eight Pacific sites (169, 170, 171, 581, 597, 800, 803, and 865), most of which have not been previously measured for paleomagnetism.

¹Sager, W.W., 2004. Data report: Paleomagnetism of basaltic rocks cored from western Pacific DSDP and ODP boreholes. *In* Sager, W.W., Kanazawa, T., and Escutia, C. (Eds.), *Proc. ODP, Sci. Results*, 191, 1-27 [Online]. Available from World Wide Web: <http://www-odp.tamu.edu/publications/191_SR/VOLUME/CHAPTERS/003.PDF>. [Cited YYYY-MM-DD]

²Department of Oceanography, Texas A&M University, College Station TX 77843-3146, USA.
wsager@ocean.tamu.edu

SAMPLE SITES

Sites 169, 170, and 171

Sites 169–171 were cored during DSDP Leg 17 in the Central Pacific. Site 169 (10.7°N, 173.6°E) is located on the abyssal seafloor ~300 km east of Mejit Island in the Marshall Islands (Shipboard Scientific Party, 1973a). Igneous rocks were recovered in four cores: diabase sills in Cores 17-169-5R and 6R (6.1 m recovered) and basalt in Cores 17-169-11R and 12R (4.0 m recovered). The igneous rocks from Site 169 have not been dated; however, the basalts from the bottom of the hole are probably crustal basalts (Bass et al., 1973), so the age can be inferred from magnetic lineations. Site 169 sits on Anomaly M21 (Nakanishi et al., 1992), which implies a date of 148 Ma using the timescale of Gradstein et al. (1994). The diabase sill is likely mid-Cretaceous in age, similar to other sills that are widespread in the western Pacific (Schlanger et al., 1981).

Site 170 was drilled on the abyssal seafloor in the Central Pacific Basin (11.8°N, 177.6°E). The only igneous rock recovered was 3.0 m of altered basalt in Core 17-170-16R (Shipboard Scientific Party, 1973b). Although the basalt has not been dated, an age can be inferred from magnetic lineations mapped in the Central Pacific Basin. Site 170 is located on Anomaly M16 (Nakanishi and Winterer, 1998), implying a date of 140 Ma (Gradstein et al., 1994).

Site 171 (19.1°N, 169.5°W) is located atop Horizon Guyot at the north end of the Line Islands chain (Shipboard Scientific Party, 1973c). Coring recovered a single basalt flow, ~3 m in thickness, from among Cenomanian limestones in Cores 17-171-26R and 27R. In addition, some basalt fragments were recovered at the bottom of the hole, in Core 17-171-33R, but no fragments were large enough for paleomagnetic sampling. Although basalt samples from Site 171 have not been dated, dredged basalt from the flanks of Horizon Guyot gave a $^{39}\text{Ar}/^{40}\text{Ar}$ total fusion date of 88.1 ± 0.4 Ma (Schlanger et al., 1984) (this and other age errors are given as 1σ).

Site 581

Site 581 (43.9°N, 159.8°E) is located on the abyssal seafloor of the northwest Pacific plate, north of Shatsky Rise. The site was cored during Legs 86 and 88. Drilling during Leg 86, Hole 581 was cored as a pilot hole for a downhole seismometer experiment conducted during Leg 88. Hole 581 was terminated after basement was struck and 3.7 m of basalt in Core 86-581-19R (Shipboard Scientific Party, 1985) was recovered. Basalt cores were recovered during Leg 88 from Holes 581A, 581B, and 581C (Shipboard Scientific Party, 1987). According to the Leg 88 *Initial Reports* volume (Shipboard Scientific Party, 1987), Hole 581A was sited 293 m south of Hole 581, whereas Hole 581B was sited 305 m north of Hole 581A, which would put it within 12 m of Hole 581, if the positioning was accurate. As is seen in the results (below), differences in magnetic polarity suggest that the holes are not that closely spaced. No details of the siting of Hole 581C were given in the Leg 88 *Initial Reports* volume. In Hole 581A, one core (88-581A-3R) was drilled into basement, recovering 4.9 m of basalt. Coring in Hole 581B recovered 15.8 m of basalt from four cores (88-581B-1R through 4R). This section was divided into 13 flows on the basis of cooling boundaries (Shipboard Sci-

entific Party, 1987). Hole 581C penetrated deepest into basement (20.6 m), recovering 16.3 m of basalt, divided into six flow units (Shipboard Scientific Party, 1987).

No accurate dating has been done for Site 581 basalts. However, an estimate of the age is possible from seafloor magnetic lineations. Site 581 is located between Anomaly M1 and another lineation that is unidentified (Nakanishi et al., 1999). From the pattern, it appears there was a ridge jump in the vicinity and the unidentified lineation is slightly older than Anomaly M1. Thus, we can estimate the age of the lineation at 124–127 Ma (Anomaly M1–M3) using the timescale of Gradstein et al. (1994).

Site 597

During DSDP Leg 92, Site 597 was drilled on abyssal seafloor in the southeast Pacific (18.6°S, 129.8°W; Shipboard Scientific Party, 1986). The site is located on Anomaly C9, which indicates the seafloor is 27.5 Ma in age (Cande and Kent, 1995). Although basalt was cored in four holes, pieces large enough to be vertically oriented were only recovered in Holes 597B and 597C. Hole 597B penetrated 24.6 m of igneous section, recovering 5.4 m, whereas Hole 597C penetrated 91 m of basement, recovering 48.5 m. Although the section was lacking clear chilled margins that indicate flow boundaries, shipboard scientists divided the section into three units based on differences in olivine content (Shipboard Scientific Party, 1986). The boundary between the upper two units, I and II, is located between Sections 92-597C-7R-5 and 8R-1 (100.5 meters below seafloor [mbsf]), whereas the boundary between Units II and III is situated in Section 10R-2 (121.3 mbsf).

Paleomagnetic measurements were conducted on Site 597 samples because it appeared that the initial shipboard studies did not include demagnetization on basalt samples to properly remove overprints and determine the characteristic magnetization direction (Shipboard Scientific Party, 1986). However, alternating-field (AF) demagnetization was performed on 69 samples, reported in another section of the Leg 92 *Initial Reports* volume (Nishitani, 1986). Although the samples were demagnetized in fields up to 90 mT, Nishitani did not explain how the characteristic remanence inclination values were calculated. Having collected additional samples and made new analyses in this study, I report the new data here and combine them with the older data.

Site 800

During Leg 129, three dolerite sill units that intruded into Berriasian sediments located on Jurassic-age abyssal seafloor in the western Pacific were cored in Hole 800A (21.9°N, 152.3°E; Shipboard Scientific Party, 1990). Approximately 7.1 m of igneous core was recovered from 46.4 m of section. These sills are probably part of a widespread mid-Cretaceous volcanic episode (Schlanger et al., 1981). A $^{39}\text{Ar}/^{40}\text{Ar}$ radiometric date of 126.1 ± 0.6 Ma was determined from Hole 800A dolerite samples (Pringle, 1992). Shipboard paleomagnetic studies used whole-core fragments and did not demagnetize above 12 mT (Shipboard Scientific Party, 1990), suggesting these preliminary results were not accurate owing to difficulties in measuring irregular core pieces and incompletely removed overprints.

Site 803

A 22.5-m section of tholeiitic basalt flows and pillow lavas was cored in Hole 803A (2.4°N, 160.5°E) on the Ontong Java Plateau during Leg 130 (Shipboard Scientific Party, 1991). Approximately 12.9 m of igneous core was recovered, and shipboard scientists divided the section into nine igneous units (Shipboard Scientific Party, 1991). A weighted average of four $^{39}\text{Ar}/^{40}\text{Ar}$ radiometric dates given in Mahoney et al. (1993) yields an age of 90.2 ± 1.2 Ma for the igneous section. No magnetic measurements have been reported from these rocks.

Site 865

Hole 865A (18.4°N, 179.6°W) was drilled into the summit of Allison Guyot in the Mid-Pacific Mountains during Leg 143 (Shipboard Scientific Party, 1993). Coring penetrated four basaltic sills, recovering 18.3 m of igneous core, but only three of the units yielded pieces suitably oriented for paleomagnetic study. A $^{39}\text{Ar}/^{40}\text{Ar}$ radiometric date of 110.7 ± 1.2 Ma was determined for these sills (Pringle and Duncan, 1995). Preliminary shipboard paleomagnetic measurements were made from large oriented core pieces (Shipboard Scientific Party, 1993) but are likely inaccurate for reasons previously stated.

METHODS AND ANALYSIS

Samples were obtained as 2.5-cm (1 in) minicores drilled perpendicular to the split face of the rock cores. Samples were taken only from hemi-cylindrical pieces long enough to ensure that they remained oriented during rotary coring. An upcore orientation mark was scribed on each sample to provide vertical orientation. Samples were spaced at irregular intervals in the core, with the object of collecting at least two to three samples from each flow unit, where units have been defined. In those cores without any igneous unit definitions, the sampling rate was one to three samples per section.

Samples were measured with the shipboard cryogenic magnetometer aboard the *JOIDES Resolution* during Leg 191. All samples were demagnetized to isolate a characteristic remanent magnetization. Typically, AF demagnetization was attempted on a subset of samples and if this procedure seemed adequate, it was used for the remainder of the samples. AF demagnetization was conducted in two different demagnetization units. Demagnetization in low fields (up to 30 mT) was conducted using the inline AF demagnetization coils mated to the shipboard cryogenic magnetometer. Because these coils may produce a spurious magnetization with high AF field values, demagnetization at fields above 30 mT was done with a separate discrete sample demagnetization unit. Usually the AF demagnetization proceeded in 5-mT steps from 10 to 40 or 50 mT and 10-mT steps up to 70 mT, but a few experiments included smaller demagnetization steps.

For some cores, thermal demagnetization methods were used when AF demagnetization apparently worked poorly. Thermal demagnetization samples underwent stepwise demagnetization beginning at 150°C and typically continuing in 50°C steps up to 450–625°C. On occasion, more detailed demagnetization experiments were conducted with 25°C steps above 400–450°C. If the sample demagnetization appeared to isolate the characteristic remanence direction at lower-temperature steps,

the demagnetization was sometimes curtailed at lower temperatures (e.g., ~450°–500°C).

Demagnetization results from each sample were plotted on an orthogonal vector diagram (Zijderveld plot) to find a characteristic magnetization direction. Using principal component analysis (Kirschvink, 1980), a least-squares line was fit to a straight segment of the demagnetization curve (if one was evident) anchored at the plot origin. The best least-squares magnetization vector was calculated, along with the maximum angle of deflection (MAD) (Kirschvink, 1980), which is a measure of the scatter in the points constraining the magnetization inversion.

Magnetization inclinations from the individual samples were combined to calculate a mean direction for the site in several steps. I used analysis methods described by Cox and Gordon (1984), which recommend working with colatitude, rather than inclination, but are otherwise analogous to inclination analysis. First, colatitude values for samples from each individual flow were averaged to determine a flow mean. Flow average colatitude values were tested against those of adjacent flows to see if they are statistically different at the 95% confidence level using the Z statistic (Kono, 1980). If adjacent means were not statistically distinct, they were combined and the procedure repeated with other adjacent flows. A few flows were sampled with a single sample, which precluded determining the standard deviation for that flow. In such cases, the average standard deviation for all flows was used for the single sample for testing the colatitude relative to surrounding flows. Using this method, a series of group means was calculated. Cox and Gordon (1984) recommend that group means representing an interval of time less than the coherency time of paleosecular variation should be combined and averaged so that oversampling of short time intervals does not bias the mean colatitude and uncertainty estimates. To accomplish this, group means were judged to be serially correlated if they did not show a large change between successive means (~8° to 10°) or if a group of colatitudes followed a smooth trend (Cox and Gordon, 1984). Although this procedure is subjective, the result is a more conservative estimate of the mean colatitude, the number of independent flow mean colatitudes, and the error limits.

Using the independent group mean colatitude values, the site mean value was computed, again following the methods of Cox and Gordon (1984). This procedure both provides a correction for bias caused by averaging inclination-only data and gives an estimate of the data errors and site mean colatitude. The mean colatitude is calculated by averaging the group means and applying a correction for bias from inclination-only data. An estimate of the random error is determined from between-group colatitude variations, and an estimate of the colatitude variance produced by secular variation is taken from a model of secular variation. The final error bounds are calculated including an assumption of 2° of systematic error possibly caused by off-vertical tilt of the borehole (a quantity not measured during most legs) and correcting for the number of independent group means (Cox and Gordon, 1984).

RESULTS

Site 169

Sixteen samples were measured from Site 169, with six from the diabase and the other ten from the basement basalt (Table T1). Natural

T1. Paleomagnetic data for igneous samples, Leg 17, p. 19.

remanent magnetization (NRM) intensities were higher in the basalt section (1.9–7.3 A/m) than in the diabase (0.7–1.9 A/m). All samples were AF demagnetized. Demagnetization behavior for the basalts was generally excellent, with successive demagnetization steps tracing a smooth line toward the origin (Fig. F1). Because of this behavior, MAD angles were small, typically $<2^\circ$ (Table T1). Although the results from the diabase sill were not quite as consistent, as indicated by larger MAD angles (2.9° – 5.6°), it was possible to define characteristic magnetization directions for all samples (Table T1).

All inclinations from the diabase sill are negative and define two distinct units. The upper four samples (17-169-6R-1, 27–29 cm, to 6R-4, 54–56 cm) yield an average colatitude of 123.7° , whereas the lower two samples (17-169-6R-4, 99–101 cm, and 6R-5, 49–51 cm) give an average of 106.8° . This difference suggests that there are two sills, probably emplaced at times separated by at least a few thousand years, long enough for secular variation to change the magnetic field inclination. If the sills were formed during the mid-Cretaceous, their magnetic polarity should be normal. The colatitude values are consistent with normal magnetization acquired south of the equator.

Two of the samples from the basalt flow section have positive inclinations. This is likely a result of inadvertent inversion of the core pieces during handling. This section could be interpreted as normal polarity formed south of the equator or a reversed polarity formed north of the equator if the inclinations of these samples are assumed to be negative. Given that the site is near Anomaly M21 and the observation that Jurassic paleomagnetic data probably indicate significantly less northward drift of the Pacific plate than mid-Cretaceous data (Cox and Gordon, 1984; Larson et al., 1992), the reversed polarity interpretation may be the correct one. The sample colatitudes fall into two groups: the upper six samples with colatitudes $<113^\circ$, and the lower four samples with colatitudes $>118^\circ$ (Table T1). The Z-test indicates that these two groups are statistically distinct at 95% confidence.

Calculation of corrected colatitudes and confidence limits gives $115.2^\circ \pm 17.8^\circ$ (this and other colatitude errors are 2σ bounds, approximating 95% confidence) for the diabase sills and $117.9^\circ \pm 16.6^\circ$ for the basalt section (Table T2).

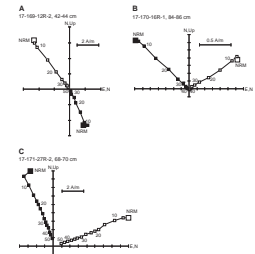
Site 170

Seven samples were measured from Core 17-170-16R (Table T1), recording moderate NRM intensities (1.1–4.2 A/m). Although the samples gave good demagnetization results (Fig. F1), the sample inclinations are inconsistent in sign. Four samples gave negative inclinations, whereas three gave positive values. Because the demagnetization results appear consistent, I assume the difference in signs reflects inversion during handling or transport and that the negative inclination is appropriate. This corresponds to a normal polarity magnetization acquired south of the equator. When given the same inclination signs, the samples show little variation in colatitude values, implying a single magnetic unit. Averaging of the colatitude values gives a mean of $103.5^\circ \pm 19.8^\circ$ (Table T2).

Site 171

Twelve samples were measured from Site 171 (Table T1). NRM values were slightly higher than those from Sites 169 and 170, ranging from

F1. Orthogonal vector plots for basalt, Leg 17, p. 12.



T2. Colatitude results for Pacific basalt core data, p. 20.

3.3 to 7.2 A/m. All produced smooth demagnetization plots (Fig. F1) and consistent negative inclinations that imply a single magnetic unit. The measurements define a mean colatitude of $101.9^\circ \pm 22.0^\circ$ (Table T2).

Site 581

A total of 84 samples from Site 581 was measured: 8 from Hole 581, 10 from Hole 581A, 28 from Hole 581B, and 38 from Hole 581C (Table T3). In general, NRM values were moderate to strong but display a range from 1.4 to 13.9 A/m. Only 10 samples were AF demagnetized because the samples appeared to be prone to acquisition of a spurious magnetization, perhaps an anhysteretic remanent magnetization (ARM), induced in the demagnetization apparatus at high demagnetization steps. Demagnetization behavior of Site 581 samples was not as smooth as those from Sites 169–171; although only three samples displayed unstable behavior. Commonly, the demagnetization removed a moderate to large low-temperature overprint and sometimes a separate medium-temperature overprint (Fig. F2). The characteristic magnetization direction was typically revealed at temperatures of 300°C and above (Fig. F2). Typically, four to six demagnetization steps were used to calculate the characteristic direction, producing relatively low MAD angles of less than $\sim 8^\circ$ (Table T3).

Because the four holes were drilled within $\sim 300\text{--}400$ m of one another but with relative positions that are not well known, it was necessary to compare the results from each hole and combine them. Samples from both Holes 581 and 581A were from a single core each, and from consistent positive inclinations, each appear to be a single magnetic unit (Table T3; Fig. F3). Inclinations from Hole 581C samples are likewise predominantly positive and can be subdivided into three units (Table T3). The positive inclinations in these cores imply a normal magnetization formed north of the equator. In contrast, Hole 581B inclinations are predominantly negative, implying reversed polarity. Furthermore, variations between flows imply eight statistically distinct units (Table T3). Three of the units are defined by only one sample each. Although Cox and Gordon (1984) used one-sample units in their analyses, it is possible that some of these samples gave spurious results so I took a more conservative approach and ignored these three data points.

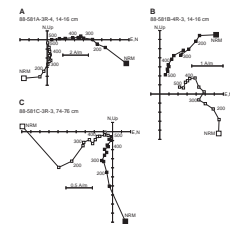
Although Site 581 produced 13 statistically distinct magnetic groups (Fig. F3), differences between group means are not great in most sections. For calculations to determine a site mean, group means in Holes 581B and 581C were recombined. All of the means from Hole 581C were combined into a single value, whereas Hole 581B data were assimilated in two units (Fig. F3). With the two units from Holes 581 and 581A, the estimated total number of independent units is five (Table T2). Using the corresponding normal polarity colatitudes for reversed polarity data from Hole 581B, a site mean of $82.9^\circ \pm 9.8^\circ$ was calculated (Table T2).

Site 597

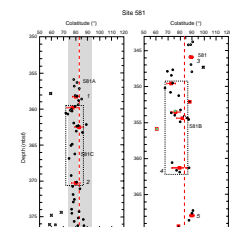
In this study, 109 samples were measured from Site 597, with 14 from Hole 597B and 95 from Hole 597C. This augments 69 measurements published by Nishitani (1986). Surprisingly, a large number of samples (27) gave scattered demagnetization results, from which it was

T3. Paleomagnetic data for igneous samples, Site 581, p. 21.

F2. Orthogonal vector plots for basalt, Site 581, p. 13.



F3. Colatitude data, Site 581, p. 14.



impossible to define a characteristic direction (Table T4). Moreover, with many samples it was impossible to define the characteristic magnetization direction with more than three to four demagnetization steps (Table T4). It is not clear why the samples in this study gave erratic results: whether the problem occurred in measurement or in the 17 years of storage, or whether Nishitani, who also used AF demagnetization, simply did not mention spurious results in his report. Interestingly, all of the unstable samples are from Hole 597C, suggesting the erratic behavior is at least partly dependent on lithology.

Despite these problems, the best demagnetization data yield smooth orthogonal vector plots (Fig. F4) that define consistent magnetization vectors. Most samples give positive inclinations, indicative of reversed magnetic polarity in the Southern Hemisphere, where the site is located. NRM values are somewhat low, with most samples having magnetizations <3 A/m.

Most samples give consistent colatitude values, although it was necessary to exclude some apparent outlier values from group mean calculations (Table T4; Fig. F5). The outliers are unsurprising given the aforementioned difficulty with erratic demagnetization results. Statistical analysis indicates eight distinct magnetic groups with data from Hole 597B combined into a single unit with the upper 4 m of the Hole 597C basalt section. These data show that colatitude scatter is low from 100 mbsf downward, corresponding to the bottom two units defined by shipboard scientists. This observation implies that this part of the section was emplaced rapidly, with little time for secular variation to occur. In the site-mean calculations, the lowest two groups were combined (Fig. F5), giving an estimate of seven independent group means (Table T2). This produced a site mean colatitude of $119.5^\circ \pm 9.9^\circ$ (Table T2), which corresponds to a paleolatitude of 29.5°S .

Site 800

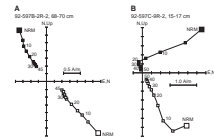
Samples from Hole 800A were the most problematic of all those measured in this study. Despite treatment using both AF and thermal demagnetization, for many samples it was impossible or difficult to define a consistent characteristic remanent magnetization direction. A few samples gave good demagnetization results (Fig. F6), but almost half (9 of 19) of the samples gave scattered results (Table T5). The fact that all of the unstable samples come from Core 129-800-58R suggests a problematic lithologic unit. This problematic behavior has been noted in studies of other mid-Cretaceous Pacific sills (e.g., Steiner, 1981).

Inclinations of the samples from Core 129-800A-57R are dominantly negative, whereas those from Cores 58R and 60R are positive. The inclinations imply a nonequatorial paleolatitude, thus implying a difference in polarity. Radiometric dates for the Site 800 sills correspond to the last polarity reversals of the M-series, so this difference in polarity implies the two groups are from sills emplaced during different polarity chrons. Other paleomagnetic data indicate that the Pacific plate has drifted $\sim 30^\circ\text{--}35^\circ$ northward since the mid-Cretaceous (Larson et al., 1992), so the negative inclinations probably formed during a normal polarity chron at a site south of the equator.

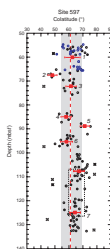
Colatitudes from Hole 800A were averaged as two independent groups, with the reversed polarity data changed to corresponding normal polarity values (Table T5; Fig. F7). The data combine to give a site-mean colatitude of $105.1^\circ \pm 17.0^\circ$ (Table T2).

T4. Paleomagnetic data for igneous samples, Site 597, p. 23.

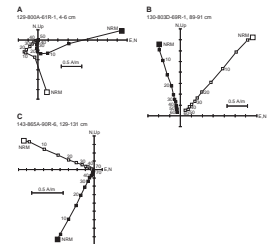
F4. Orthogonal vector plots for basalt, Site 597, p. 15.



F5. Colatitude data, Site 597, p. 16.

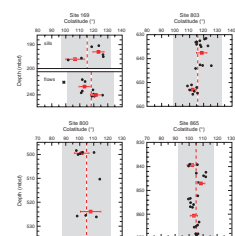


F6. Orthogonal vector plots for basalt, Sites 800, 803, and 865, p. 17.



T5. Paleomagnetic data for igneous samples, Sites 800, 803, and 865, p. 26.

F7. Colatitude data, Sites 169, 800, 803, and 865, p. 18.



Site 803

Demagnetization results from the 20 Site 803 samples were excellent, with most samples showing little overprint and giving smooth demagnetization curves (Fig. F6). Characteristic remanent magnetization directions were precisely defined, with five to seven steps used in the calculation, producing MAD angles $<2^\circ$ (Table T5). Inclination values were consistently negative, indicating a normal polarity acquired south of the equator. Colatitudes were grouped into two independent units (Fig. F7) and defined a site-mean colatitude of $116.8^\circ \pm 16.5^\circ$ (Table T2).

Site 865

Data from Site 865 also displayed consistent demagnetization behavior with little overprint (Fig. F6). Almost all of the 22 samples allowed five to seven demagnetization steps for definition of the characteristic remanent magnetization direction, often giving MAD angles of $<1^\circ$ (Table T5). All samples gave negative inclinations, indicating normal polarity sills emplaced south of the equator. This result is consistent with the radiometric date for the sites, which falls within the Cretaceous Long Normal Superchron. Mean colatitudes for the three sampled sills were distinct, averaging to give a site-mean of $104.9^\circ \pm 13.2^\circ$ (Table T2; Fig. F7).

ACKNOWLEDGMENTS

The author thanks Jerry Bode of the West Coast Core Repository for his help in sampling DSDP cores as well as Phil Rumford and the staff of the Gulf Coast Repository for their help with ODP cores. This research used samples and data provided by the Ocean Drilling Program (ODP). The ODP is sponsored by the U.S. National Science Foundation (NSF) and participating countries under the management of Joint Oceanographic Institutions (JOI), Inc. Funding from JOI/USSSP supported the measurements and analyses.

REFERENCES

- Bass, M.N., Moberly, R., Rhodes, J.M., Shih, C.C., and Church, S.E., 1973. Volcanic rocks cored in the Central Pacific, Leg 17, Deep Sea Drilling Project. *In* Winterer, E.L., Ewing, J.I., et al., *Init. Repts. DSDP*, 17: Washington (U.S. Govt. Printing Office), 429–503.
- Cande, S.C., and Kent, D.V., 1995. Revised calibration of the geomagnetic polarity timescale for the Late Cretaceous and Cenozoic. *J. Geophys. Res.*, 100:6093–6095.
- Cox, A., and Gordon, R.G., 1984. Paleolatitudes determined from paleomagnetic data from vertical cores. *Rev. Geophys. Space Phys.*, 22:47–72.
- Gordon, R.G., and Cox, A., 1980. Calculating paleomagnetic poles for oceanic plates. *Geophys. J. R. Astron. Soc.*, 63:619–640.
- Gradstein, F.M., Agterberg, F.P., Ogg, J.G., Hardenbol, J., van Veen, P., Thierry, J., and Huang, Z., 1994. A Mesozoic time scale. *J. Geophys. Res.*, 99:24051–24074.
- Kirschvink, J.L., 1980. The least-squares line and plane and the analysis of palaeomagnetic data. *Geophys. J. R. Astron. Soc.*, 62:699–718.
- Kono, M., 1980. Paleomagnetism of DSDP Leg 55 basalts and implications for the tectonics of the Pacific plate. *In* Jackson, E.D., Koizumi, I., et al., *Init. Repts. DSDP*, 55: Washington (U.S. Govt. Printing Office), 737–752.
- Larson, R.L., Steiner, M.B., Erba, E., and Lancelot, Y., 1992. Paleolatitudes and tectonic reconstructions of the oldest portion of the Pacific plate: a comparative study. *In* Larson, R.L., Lancelot, Y., et al., *Proc. ODP, Sci. Results*, 129: College Station, TX (Ocean Drilling Program), 615–631.
- Mahoney, J.J., Storey, M., Duncan, R.A., Spencer, K.J., and Pringle, M., 1993. Geochemistry and geochronology of Leg 130 basement lavas: nature and origin of the Ontong Java Plateau. *In* Berger, W.H., Kroenke, L.W., Mayer, L.A., et al., *Proc. ODP, Sci. Results*, 130: College Station, TX (Ocean Drilling Program), 3–22.
- Nakanishi, M., Sager, W.W., and Klaus, A., 1999. Magnetic lineations within Shatsky Rise, northwest Pacific Ocean: implications for hot spot–triple junction interaction and oceanic plateau formation. *J. Geophys. Res.*, 104:7539–7556.
- Nakanishi, M., Tamaki, K., and Kobayashi, K., 1992. Magnetic anomaly lineations from Late Jurassic to Early Cretaceous in the west-central Pacific Ocean. *Geophys. J. Int.*, 109:701–719.
- Nakanishi, M., and Winterer, E.L., 1998. Tectonic history of the Pacific-Farallon-Phoenix triple junction from Late Jurassic to Early Cretaceous: an abandoned Mesozoic spreading system in the Central Pacific Basin. *J. Geophys. Res.*, 103:12453–12468.
- Nishitani, T., 1986. Magnetic properties of basalt samples from Deep Sea Drilling Project Holes 597B and 597C. *In* Leinen, M., Rea, D.K., et al., *Init. Repts. DSDP*, 92: Washington (U.S. Govt. Printing Office), 527–535.
- Pringle, M.S., 1992. Radiometric ages of basaltic basement recovered at Sites 800, 801, and 802, Leg 129, western Pacific Ocean. *In* Larson, R.L., Lancelot, Y., et al., *Proc. ODP, Sci. Results*, 129: College Station, TX (Ocean Drilling Program), 389–404.
- Pringle, M.S., and Duncan, R.A., 1995. Radiometric ages of basaltic lavas recovered at Sites 865, 866, and 869. *In* Winterer, E.L., Sager, W.W., Firth, J.V., and Sinton, J.M. (Eds.), *Proc. ODP, Sci. Results*, 143: College Station, TX (Ocean Drilling Program), 277–283.
- Schlanger, S.O., Garcia, M.O., Keating, B.H., Naughton, J.J., Sager, W.W., Haggerty, J.A., Philpotts, J.A., and Duncan, R.A., 1984. Geology and geochronology of the Line Islands. *J. Geophys. Res.*, 89:11261–11272.
- Schlanger, S.O., Jenkyns, H.C., and Premoli-Silva, I., 1981. Volcanism and vertical tectonics in the Pacific Basin related to global Cretaceous transgressions. *Earth Planet. Sci. Lett.*, 52:435–449.
- Shipboard Scientific Party, 1973a. Site 169. *In* Winterer, E.L., Ewing, J.I., et al., *Init. Repts. DSDP*, 17: Washington (U.S. Govt. Printing Office), 247–262.

- , 1973b. Site 170. *In* Winterer, E.L., Ewing, J.I., et al., *Init. Repts. DSDP*, 17: Washington (U.S. Govt. Printing Office), 263–281.
- , 1973c. Site 171. *In* Winterer, E.L., Ewing, J.I., et al., *Init. Repts. DSDP*, 17: Washington (U.S. Govt. Printing Office), 283–334.
- , 1985. Site 581. *In* Heath, G.R., Burkle, L.H., et al., *Init. Repts. DSDP*, 86: Washington (U.S. Govt. Printing Office), 241–266.
- , 1986. Site 597. *In* Leinen, M., Rea, D.K., et al., *Init. Repts. DSDP*, 92: Washington (U.S. Govt. Printing Office), 25–96.
- , 1987. Site 581. *In* Duennebier, F.K., Stephen, R., Gettrust, J.F., et al., *Init. Repts. DSDP*, 88: Washington (U.S. Govt. Printing Office), 9–36.
- , 1990. Site 800. *In* Lancelot, Y., Larson, R.L., et al., *Proc. ODP, Init. Repts.*, 129: College Station, TX (Ocean Drilling Program), 33–89.
- , 1991. Site 803. *In* Kroenke, L.W., Berger, W.H., Janecek, T.R., et al., *Proc. ODP, Init. Repts.*, 130: College Station, TX (Ocean Drilling Program), 101–176.
- , 1993. Site 865. *In* Sager, W.W., Winterer, E.L., Firth, J.V., et al., *Proc. ODP, Init. Repts.*, 143: College Station, TX (Ocean Drilling Program), 111–180.
- Steiner, M.B., 1981. Paleomagnetism of the igneous complex, Site 462. *In* Larson, R. L., Schlanger, S.O., et al., *Init. Repts. DSDP*, 61: Washington (U.S. Govt. Printing Office), 717–729.

Figure F1. Orthogonal vector (Zijderveld) plots of demagnetization behavior of representative basalt samples from Leg 17. **A.** Site 169. **B.** Site 170. **C.** Site 171. Points denote projection of magnetization vector end-point on two planes, one horizontal (oriented north and east; solid symbols) and one vertical (oriented up and north; open symbols). Natural remanent magnetization (NRM) represents the undemagnetized vector. Demagnetization steps are labeled in milliTeslas.

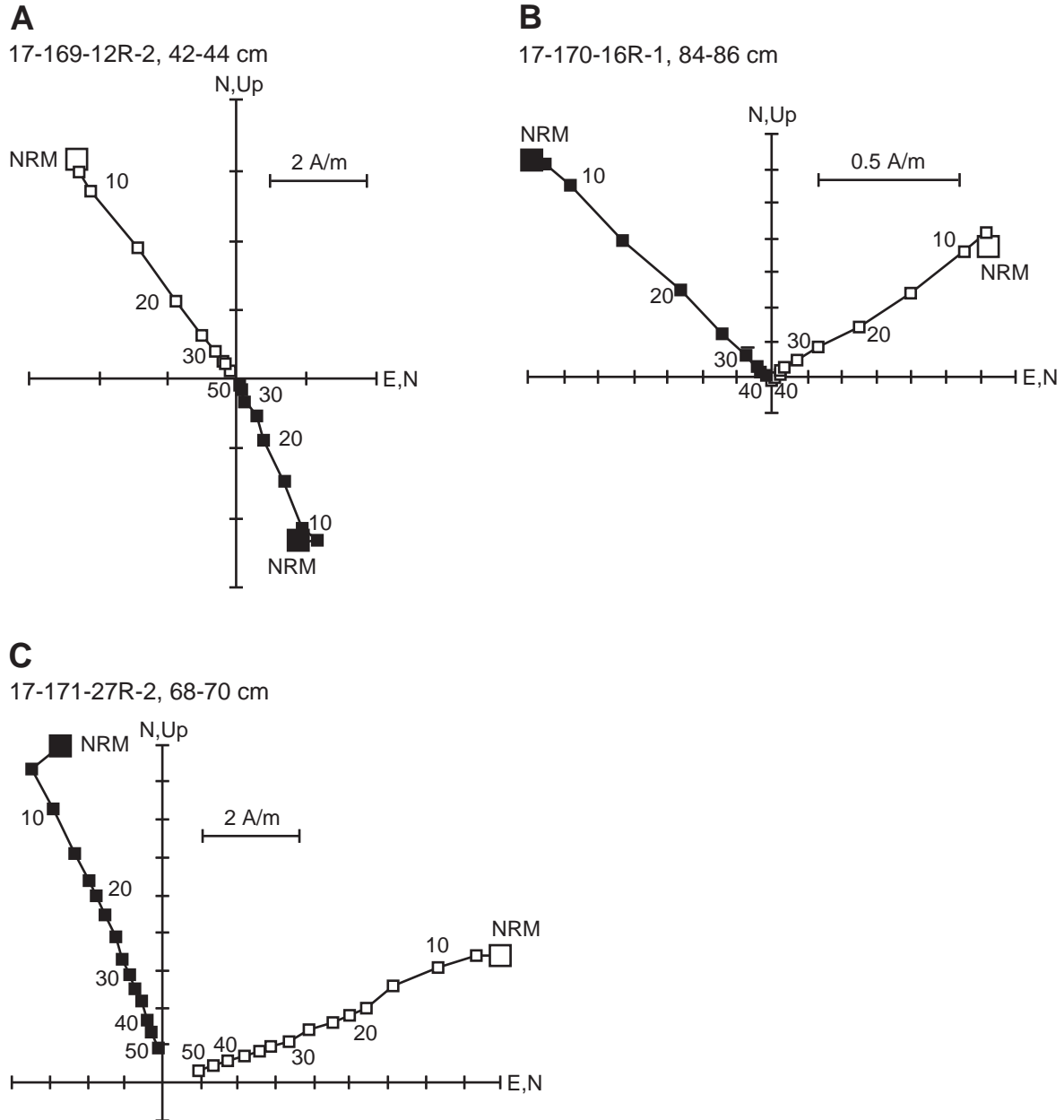


Figure F2. Orthogonal vector plots for representative basalt samples from Site 581. **A.** Hole 581A. **B.** Hole 581B. **C.** Hole 581C. Points denote projection of magnetization vector endpoint on two planes, one horizontal (oriented north and east; solid symbols) and one vertical (oriented up and north; open symbols). Natural remanent magnetization (NRM) represents the undemagnetized vector. Temperatures labeled in degrees Centigrade.

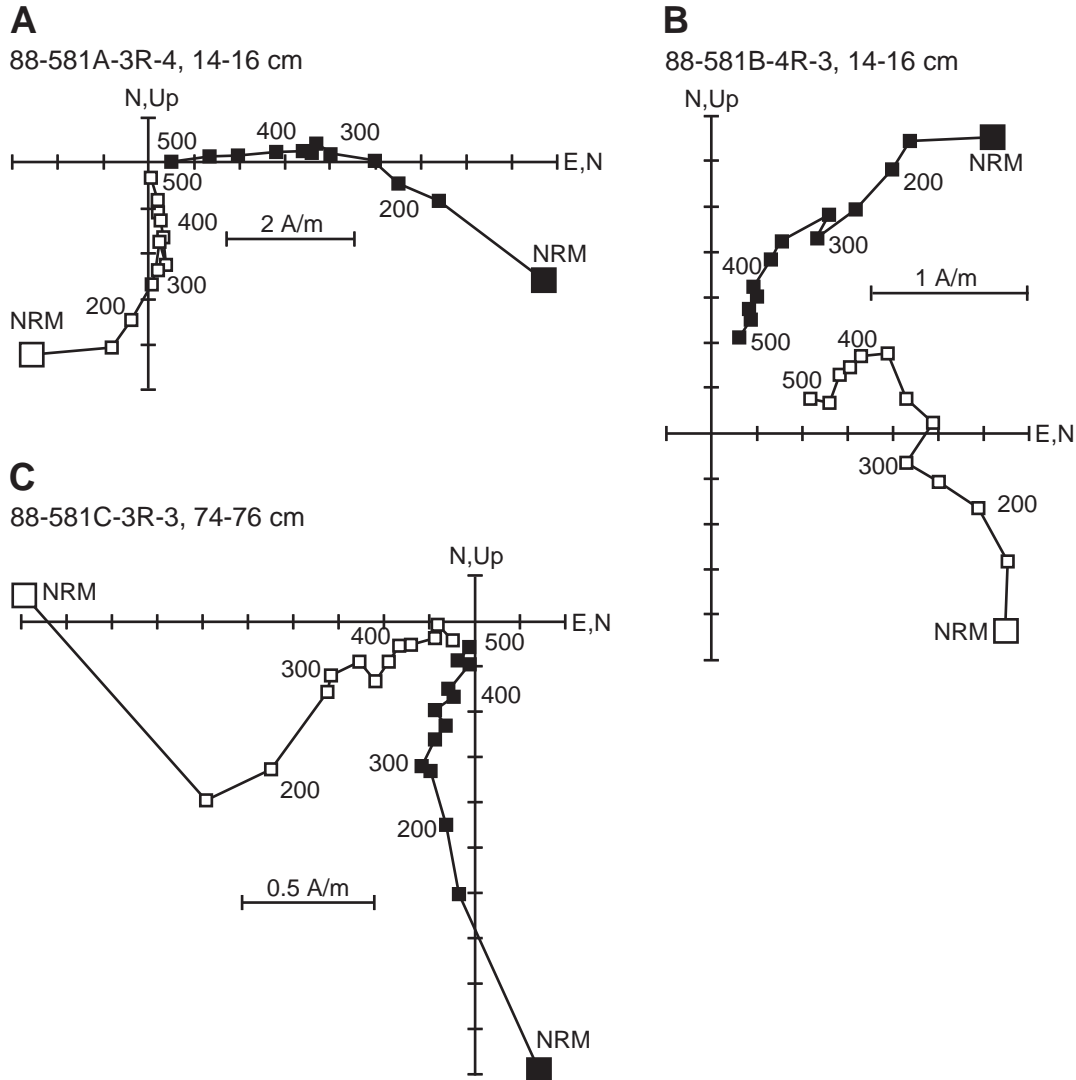


Figure F3. Colatitude data for Site 581. Left plot: open symbols = Hole 581A, solid symbols = Hole 581C. Right plot: open symbols = Hole 581, solid symbols = Hole 581B. Open red squares = three samples, which are the only samples from each respective flow and appear to be statistically distinct from neighboring flows. As discussed in the text, these three data points were not used in determining the site mean. Dotted boxes = group means combined for the site-mean calculations (see text). Numbers in italics = identifiers of the five groups considered independent. Symbols with "X" = a colatitude value not used to calculate mean colatitude. Red solid squares = group mean colatitudes, horizontal bars = one standard deviation. Red dashed lines = the mean colatitude, gray vertical bar = 95% confidence limits.

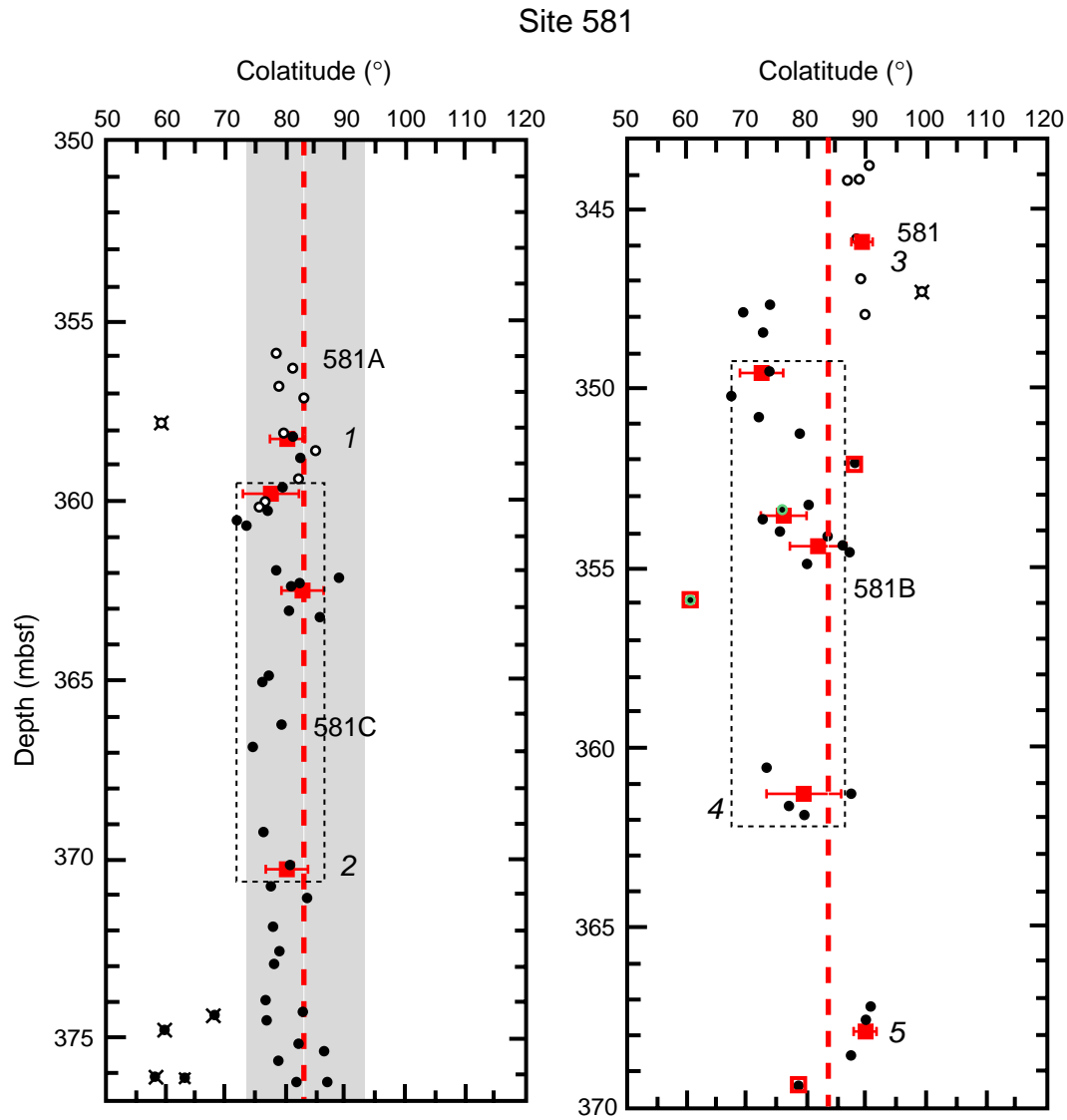


Figure F4. Orthogonal vector plots for representative basalt samples from Site 597. **A.** Hole 597B. **B.** Hole 597C. Points denote projection of magnetization vector endpoint on two planes, one horizontal (oriented north and east; solid symbols) and one vertical (oriented up and north; open symbols). Natural remanent magnetization (NRM) represents the undemagnetized vector. Demagnetization steps are labeled in milli-Teslas.

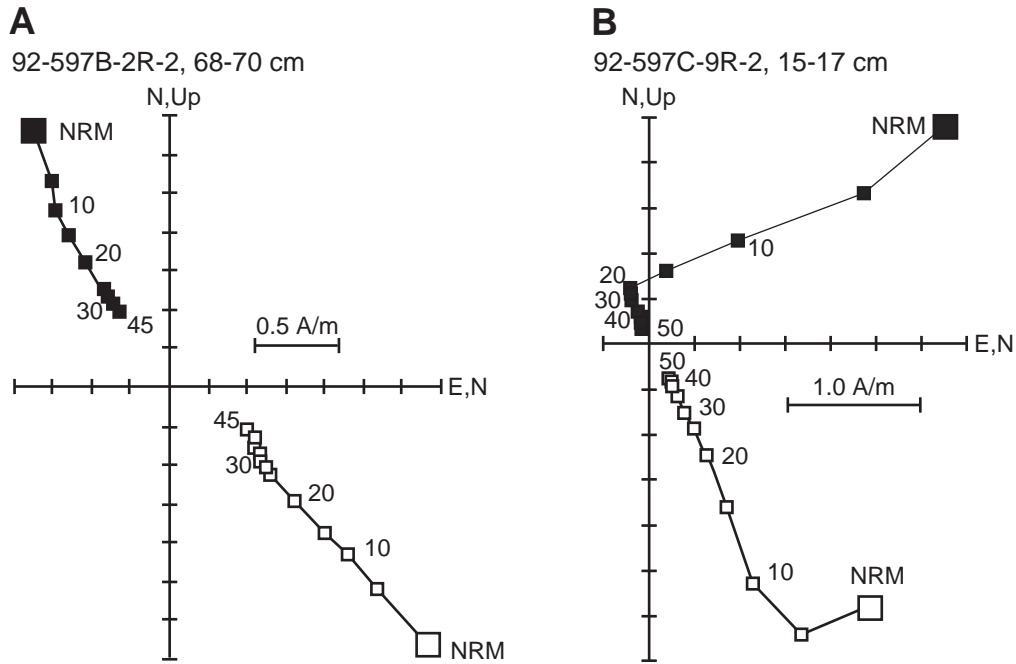


Figure F5. Colatitude data for Site 597. Open symbols = data from Nishitani (1986), solid symbols = data from this study. Blue symbols = Hole 597B, black symbols = Hole 597C. Dotted boxes = group means combined for the site-mean calculations (see text). Numbers in italics = identifiers of the five groups considered independent. Symbols with "X" = a colatitude value not used to calculate mean colatitude. Red solid squares = group mean colatitudes, horizontal bars = one standard deviation. Red dashed line = the mean colatitude, gray vertical bar = 95% confidence limits.

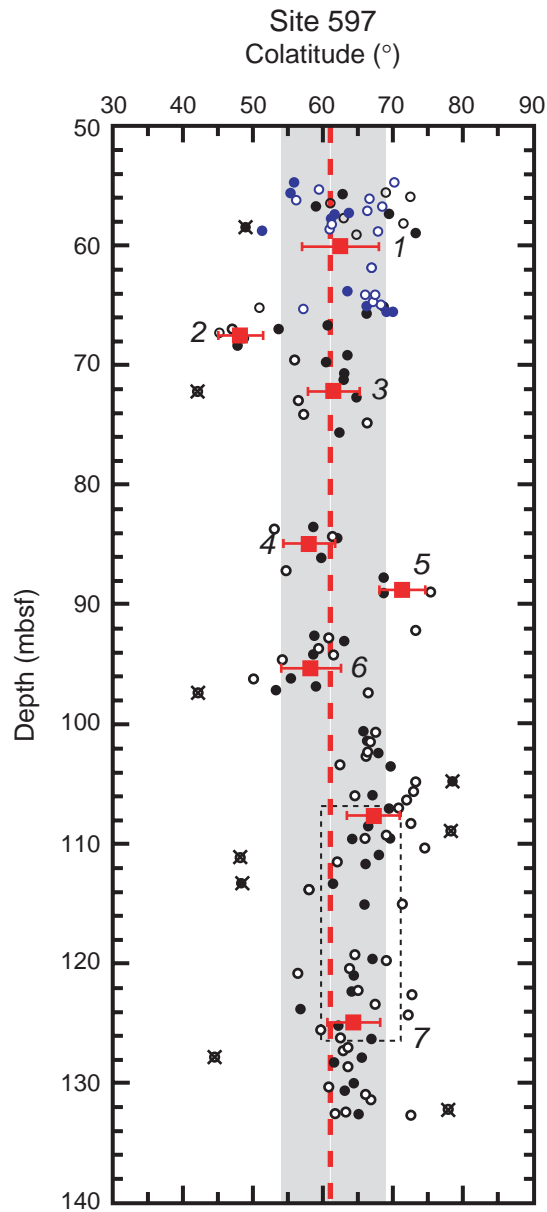


Figure F6. Orthogonal vector plots for representative basalt samples. A. Site 800. B. Site 803. C. Site 865. Points denote projection of magnetization vector endpoint on two planes, one horizontal (oriented north and east; solid symbols) and one vertical (oriented up and north; open symbols). Natural remanent magnetization (NRM) represents the undemagnetized vector. Demagnetization steps are labeled in milliTeslas.

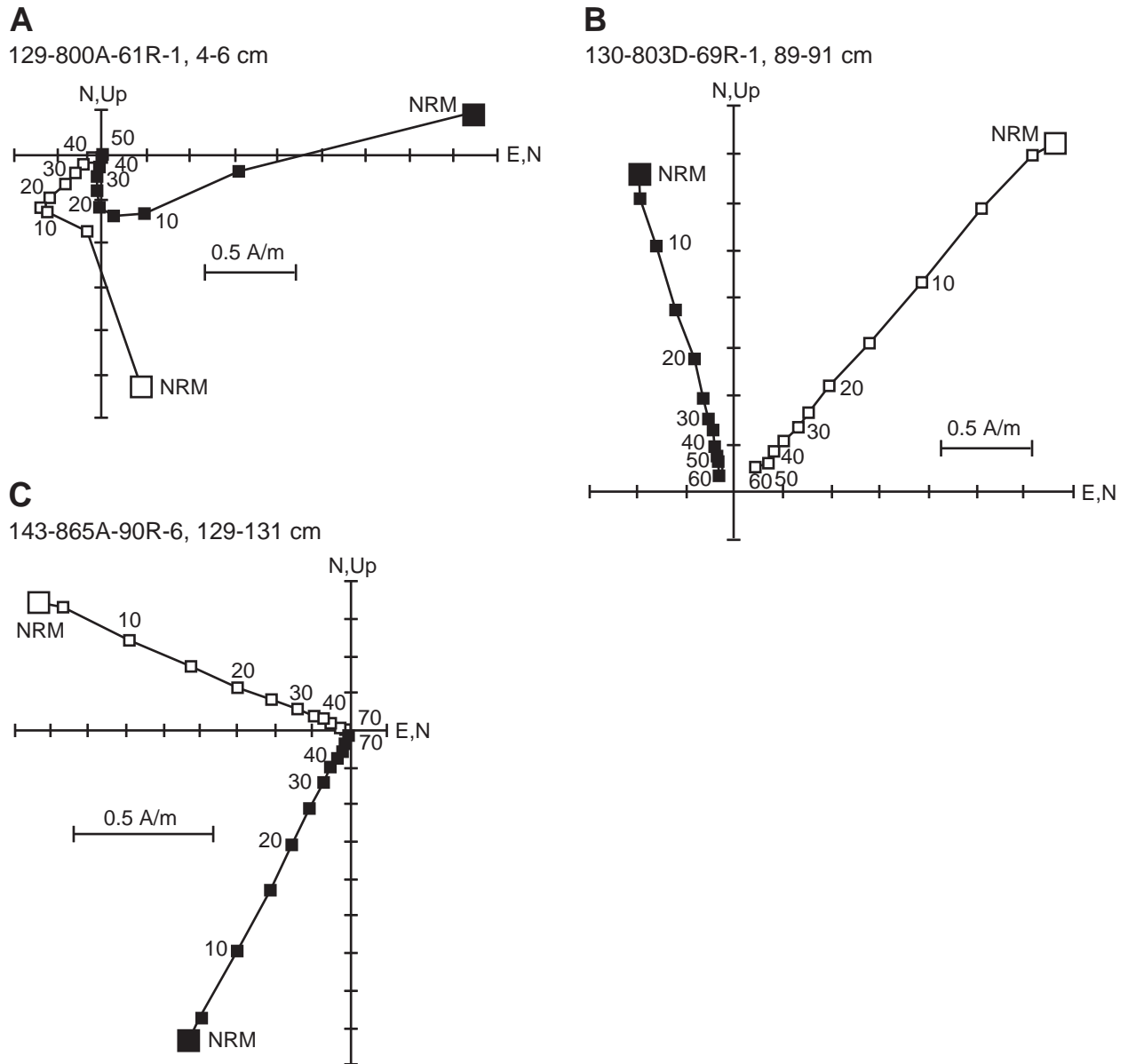


Figure F7. Colatitude data for Sites 169, 800, 803, and 865. The vertical axis in each plot = downhole depth, the horizontal axis = colatitude. The scales are identical in each plot. Solid circles = colatitude values (see Tables T1, p. 19, and T5, p. 26). Symbol with "X" = a colatitude value not used to calculate mean colatitude. Red solid squares = group mean colatitudes, horizontal bars = one standard deviation. Red dashed lines = the mean colatitude, gray vertical bars = 95% confidence limits.

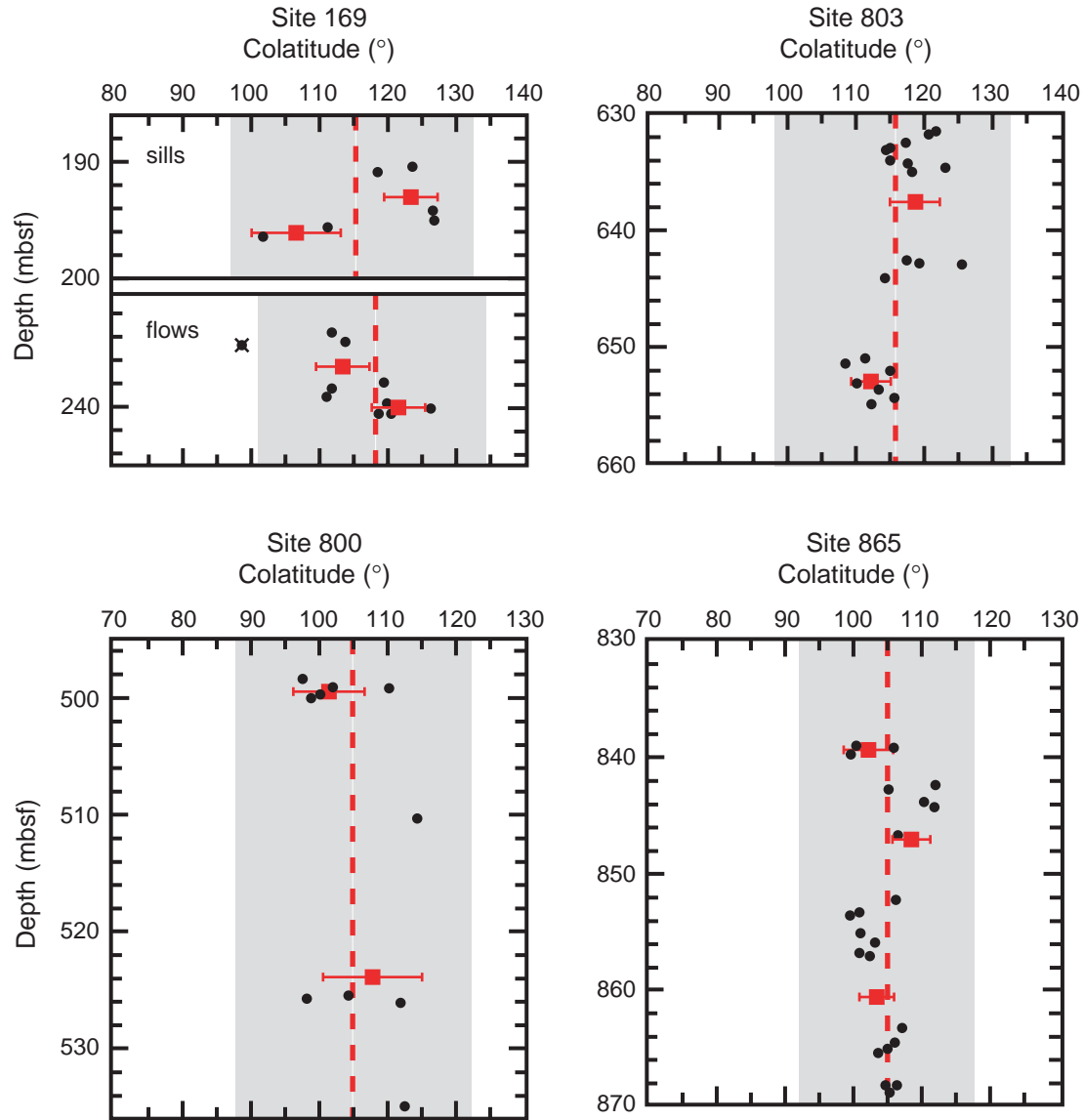


Table T1. Paleomagnetic data for igneous samples, Leg 17.

Core, section, interval (cm)	Depth (mbsf)	NRM (A/m)	Inc (°)	Demag	N	Steps	MAD (°)	Colatitude (°)	Group number	Mean colat	Std	N colat
169- (sills)												
6-1, 27	190.27	0.7	-52.9	A	4	15-40	4.5	123.5				
6-1, 98	190.98	1.4	-46.7	A	4	15-40	4.4	118.0				
6-3, 123	194.23	1.4	-56.2	A	3	35-45	5.1	126.7				
6-4, 54	195.04	0.9	-55.9	A	4	35-50	4.1	<u>126.5</u>	1	<u>123.7</u>	<u>4.1</u>	<u>4</u>
6-4, 99	195.49	2.2	-38.1	A	5	20-40	2.9	111.4				
6-5, 49	196.49	1.9	-23.3	A	6	25-50	5.6	<u>102.2</u>	2	<u>106.8</u>	<u>6.5</u>	<u>2</u>
169- (basalt flow)												
11-1, 82	233.82	5.9	38.7 [†]	A	6	25-50	2.9	111.8				
11-1, 113	234.13	2.3	-40.7	A	5	15-35	3.9	113.3				
11-1, 140	234.40	2.8	17.1 [†]	A	4	10-25	1.4	98.7*				
12-1, 2	238.02	2.1	-48.6	A	5	15-35	1.9	119.6				
12-1, 36	238.36	1.9	-38.3	A	4	15-30	2.9	111.6				
12-1, 133	239.33	5.4	-37.6	A	4	40-60	2.6	<u>111.1</u>	1	<u>113.5</u>	<u>3.5</u>	<u>5</u>
12-2, 42	239.92	7.3	-49	A	5	20-40	2.1	119.9				
12-2, 49	239.99	4.3	-55.5	A	4	15-30	2.5	126.0				
12-2, 77	240.27	5.4	-49.7	A	5	20-40	1.1	120.5				
12-2, 110	240.60	3.9	-47.8	A	5	20-40	1.0	<u>118.9</u>	2	<u>121.3</u>	<u>3.2</u>	<u>4</u>
170-												
16-1, 84	192.84	1.1	-26.7	A	6	25-50	1.7	104.1				
16-1, 93	192.93	2.6	22.7 [†]	A	6	18-35	2.1	101.8				
16-1, 107	193.07	4.2	25.6 [†]	A	6	18-30	1.7	103.5				
16-2, 25	193.75	3.0	-30.3	A	7	20-40	2.1	106.3				
16-2, 56	194.06	3.5	-26.3	A	5	15-35	1.2	103.9				
16-2, 85	194.35	2.3	-27.2	A	6	15-30	3.2	104.4				
16-2, 122	194.72	1.8	18.3 [†]	A	5	15-28	6.2	<u>99.4</u>	1	<u>103.3</u>	<u>2.2</u>	<u>7</u>
171-												
27-1, 46	334.46	4.2	-17.5	A	6	30-50	0.9	99.0				
27-1, 68	334.68	5.2	-23.4	A	8	25-70	2.2	102.2				
27-1, 109	335.09	4.8	-25.8	A	5	32-50	1.2	103.6				
27-1, 144	335.44	3.3	-35.5	A	5	22-32	1.3	109.6				
27-2, 12	335.62	3.3	-22.4	A	5	32-50	0.9	101.6				
27-2, 68	336.18	6.8	-17.9	A	5	28-40	0.9	99.2				
27-2, 115	336.65	7.2	-17.2	A	5	30-45	1.3	98.8				
27-2, 138	336.88	6.4	-18.6	A	5	32-50	0.6	99.6				
27-3, 34	337.34	4.0	-19.9	A	5	32-50	1.4	100.3				
27-3, 43	337.43	2.8	-26.2	A	6	30-50	0.9	103.8				
27-3, 72	337.72	3.9	-16.4	A	6	28-45	0.7	98.4				
27-3, 103	338.03	4.2	-26.6	A	7	30-70	1.9	<u>104.1</u>	1	<u>101.7</u>	<u>3.3</u>	<u>12</u>

Notes: NRM = natural remanent magnetization. Inc = inclination of characteristic remanent magnetization determined by principal component analysis. Demag = demagnetization. A = alternating field. N = number of measurements used for principal component analysis. Steps = demagnetization steps used for principal component analysis. MAD = maximum angle of deviation (Kirshvink, 1980). Mean colat = group mean colatitude. Std = standard deviation of group mean colatitude. N colat = number of colatitudes used to calculate group mean. * = datum not used in average colatitude calculations. Group averages are shown at the far right; underscores show the division of groups. † = sample showing anomalous inclinations (see text).

Table T2. Colatitude results for Pacific basalt core data.

Site	Mean colatitude (°)	95% confidence (°)	Lithologic units (N)	Magnetic units (N)	Polarity
169 (sill)	115.2	17.8	2	2	N
169 (flows)	117.9	16.6	2	2	N
170	103.5	19.8	1	1	N
171	101.9	22.0	1	1	N
581	82.9	9.8	13	5	N/R
597	119.5	9.9	8	7	R
800	105.1	17.0	2	2	N/R
803	116.8	16.4	3	2	N
865	104.9	13.2	4	3	N

Notes: Lithologic units = flows, sills, etc. N = normal, R = reversed.

Table T3. Paleomagnetic data for igneous samples, Site 581. (See table notes. Continued on next page.)

Core, section, interval (cm)	Depth (mbsf)	NRM (A/m)	Inc (°)	Demag	N	Steps	MAD (°)	Colatitude (°)	Group number	Mean colat	Std	N colat
581-												
19-1, 72	343.72	1.2	-0.5	T	7	350-500	7.0	90.2				
19-1, 108	344.08	2.5	2.9	T	4	375-450	3.7	88.6				
19-1, 116	344.16	1.0	6.9	T	6	375-500	3.4	86.5				
19-2, 123	345.73	2.0	3.7	A	4	15-30	1.0	88.1				
19-3, 90	346.90	3.9	2.6	A	4	10-35	1.5	88.7				
19-3, 127	347.27	2.4	-17.2	T	4	200-375	10.8	98.8*				
19-4, 19	347.69	4.1	Unstable	T								
19-4, 36	347.86	3.6	0.6	A	4	10-25	1.2	<u>89.7</u>	1	<u>88.6</u>	<u>1.3</u>	<u>6</u>
581A-												
3-1, 38	355.88	2.8	23.0	T	5	400-500	4.3	78.0				
3-1, 86	356.36	3.5	17.2	T	5	300-475	8.1	81.2				
3-1, 126	356.76	2.7	21.9	T	6	350-500	5.2	78.6				
3-2, 11	357.11	6.8	14.2	T	6	325-450	6.2	82.8				
3-2, 81	357.81	7.9	50.1	T	6	350-475	8.9	59.1*				
3-2, 111	358.11	13.9	20.6	A	7	20-50	2.1	79.4				
3-3, 8	358.58	5.5	10.3	T	6	375-500	5.7	84.8				
3-3, 92	359.42	2.7	15.7	T	3	350-400	5.8	82.0				
3-3, 147	359.97	5.1	26.1	T	5	250-375	5.4	76.2				
3-4, 14	360.14	6.4	27.6	T	6	375-500	2.2	<u>75.4</u>	1	<u>79.8</u>	<u>3.1</u>	<u>9</u>
581B- (negative inclinations assumed reversed polarity)												
1-1, 19	347.69	1.0	-30.0	T	5	375-500	5.7	73.9				
1-1, 93	348.43	0.8	-32.2	T	6	375-500	5.8	72.5				
2-1, 35	347.85	2.3	-36.2	T	5	375-500	6.5	69.9				
2-1, 55	349.55	0.8	-30.2	T	4	425-500	6.8	73.8				
2-1, 121	350.21	1.3	-39.3	T	4	400-475	7.2	67.7				
2-2, 28	350.78	1.7	-32.5	T	5	375-475	8.7	72.3				
2-2, 76	351.26	1.5	-20.8	T	4	375-450	4.2	<u>79.2</u>	1	<u>107.2</u>	<u>3.6</u>	<u>7</u>
2-3, 7	352.07	1.1	-3.6	T	4	375-450	5.7	<u>88.2*</u>	2	<u>91.8</u>		<u>1</u>
2-3, 127	353.27	4.0	-18.3	T	6	375-500	3.2	80.6				
2-3, 142	353.42	8.8	-26.1	T	4	425-500	6.6	76.2				
2-4, 18	353.68	2.5	-31.9	T	5	400-500	6.0	<u>72.7</u>	3	<u>103.5</u>	<u>4.0</u>	<u>3</u>
2-4, 52	354.02	3.1	-27.0	T	4	375-450	5.7	75.7				
2-4, 60	354.10	3.7	-12.6	T	6	375-500	6.3	83.6				
2-4, 91	354.41	4.3	-7.3	T	6	375-500	2.2	86.3				
2-4, 107	354.57	2.1	-5.5	A	4	30-45	8.0	87.2				
2-4, 140	354.90	3.3	-19.0	T	5	375-475	5.9	<u>80.2</u>	4	<u>97.4</u>	<u>4.7</u>	<u>5</u>
2-5, 91	355.91	4.7	-48.8	T	4	425-500	5.6	<u>60.3*</u>	5	<u>119.7</u>		<u>1</u>
2-5, 123	356.23	4.4	Unstable	T								
2-5, 133	356.33	6.6	Unstable	T								
3-2, 33	360.63	2.1	-30.8	T	4	425-500	11.4	73.4				
3-2, 105	361.35	3.9	-4.5	T	5	325-500	8.9	87.7				
3-2, 137	361.67	2.8	24.5 [†]	A	5	15-35	1.8	77.2				
3-3, 12	361.92	3.4	-19.5	A	4	35-50	14.4	<u>80.0</u>	6	<u>100.4</u>	<u>6.1</u>	<u>4</u>
4-1, 76	367.06	1.4	-1.9	A	5	25-45	5.3	89.1				
4-1, 130	367.60	2.8	0.4	A	6	20-45	2.6	<u>89.8</u>				
4-2, 71	368.51	6.0	5.6	A	4	20-40	2.0	<u>87.2</u>	7	<u>89.3</u>	<u>1.9</u>	<u>3</u>
4-2, 139	369.19	2.0	Unstable	T								
4-3, 14	369.44	2.7	-22.9	T	5	400-500	4.7	<u>78.1*</u>	8	<u>101.9</u>		<u>1</u>
581C-												
1-1, 68	358.28	5.1	16.7	T	5	200-350	2.5	81.5				
1-1, 120	358.80	5.6	14.7	T	4	425-500	4.3	82.5				
2-1, 7	359.67	5.5	-19.8 [†]	T	4	425-500	5.1	79.8				
2-1, 71	360.31	3.9	24.1	T	5	350-450	3.9	77.4				
2-1, 98	360.58	5.1	32.8	T	5	375-475	6.2	72.1				
2-1, 117	360.77	5.3	31.2	T	6	375-500	3.4	<u>73.2</u>	1	<u>77.7</u>	<u>4.3</u>	<u>6</u>
2-2, 85	361.95	3.9	22.2	T	8	325-500	2.9	78.5				
2-2, 104	362.14	2.7	-2.2 [†]	T	5	375-475	5.6	88.9				
2-2, 124	362.34	4.3	14.8	T	4	325-400	1.5	82.5				
2-2, 132	362.42	7.0	-17.7 [†]	T	4	350-425	5.8	80.9				
2-3, 48	363.08	5.0	18.2	T	6	350-475	1.7	80.7				
2-3, 68	363.28	4.0	8.0	T	6	325-450	3.1	86.0				
2-3, 109	363.69	5.2	15.2	T	5	375-475	1.2	<u>82.3</u>	2	<u>82.8</u>	<u>4.3</u>	<u>7</u>
2-4, 79	364.89	3.2	24.1	T	6	300-425	9.7	77.4				
2-4, 100	365.10	6.0	26.1	T	4	250-325	8.2	76.2				
2-4, 121	365.31	3.7	Unstable	T								
2-5, 28	365.88	4.3	Unstable	T								
2-5, 62	366.22	3.4	-20.9 [†]	T	4	400-475	6.9	79.2				

Table T3 (continued).

Core, section, interval (cm)	Depth (mbsf)	NRM (A/m)	Inc (°)	Demag	N	Steps	MAD (°)	Colatitude (°)	Group number	Mean colat	Std	N colat
2-5, 125	366.85	3.4	28.9	T	4	300-375	7.7	74.6				
3-1, 42	369.22	3.4	26.1	T	5	325-425	2.6	76.2				
3-1, 141	370.21	1.9	18.5	T	6	350-475	4.9	80.5				
3-2, 54	370.84	3.5	23.8	T	6	300-425	4.0	77.6				
3-2, 81	371.11	1.9	12.4	T	6	300-425	3.3	83.7				
3-3, 14	371.94	3.5	22.9	T	8	300-475	2.7	78.1				
3-3, 74	372.54	1.7	20.4	T	6	275-400	5.0	79.5				
3-3, 110	372.90	2.0	23.1	T	6	325-500	6.7	78.0				
3-4, 66	373.96	4.9	25.4	T	5	400-500	3.9	76.6				
3-4, 99	374.29	3.6	13.4	T	5	375-500	2.4	83.2				
3-4, 107	374.37	7.2	39.3	T	6	350-475	4.0	67.7*				
3-4, 116	374.46	9.3	25.1	T	5	375-500	1.7	76.8				
3-4, 141	374.71	4.3	49.3	T	6	350-475	1.9	59.8*				
3-5, 27	375.07	3.8	14.8	T	4	375-475	2.1	82.5				
3-5, 60	375.40	8.1	6.9	T	6	375-500	6.3	86.5				
3-5, 80	375.60	2.6	21.3	T	4	325-400	4.9	79.0				
3-5, 127	376.07	4.2	51.2	T	5	300-400	2.1	58.1*				
3-5, 132	376.12	2.5	45.6	T	4	325-400	3.5	63.0*				
3-5, 137	376.17	3.2	15.8	T	5	325-425	4.1	81.9				
3-5, 141	376.21	3.3	6.2	T	4	300-375	1.1	<u>86.9</u>	<u>3</u>	<u>80.0</u>	<u>3.6</u>	<u>19</u>

Notes: NRM = natural remanent magnetization. Inc = inclination of characteristic remanent magnetization determined by principal component analysis. Demag = demagnetization. A = alternating field, T = thermal. N = number of measurements used for principal component analysis. Steps = demagnetization steps used for principal component analysis. MAD = maximum angle of deviation (Kirshvink, 1980). Mean colat = group mean colatitude. Std = standard deviation of group mean colatitude. N colat = number of colatitudes used to calculate group mean. * = datum not used in average colatitude calculations. Group averages are shown at the far right; underscores show the division of groups. † = sample showing anomalous inclinations (see text).

Table T4. Paleomagnetic data for igneous samples, Site 597. (See table notes. Continued on next two pages.)

Core, section, interval (cm)	Depth (mbsf)	NRM (A/m)	Inc (°)	Demag	N	Steps	MAD (°)	Colatitude (°)	Group number	Mean colat	Std	N colat
597B-												
2-1, 20	54.49	2.8	53.3	A				56.1				
2-1, 28 [‡]	54.57	1.4	35.0	A	4	20-30	7.4	70.7				
2-1, 80 [‡]	55.17	1.1	49.2	A	4	15-28	1.9	59.9				
2-1, 91 [‡]	55.88	0.5	40.1	A	4	20-30	12.3	67.2				
2-1, 95	55.24	2.7	53.6	A				55.9				
2-2, 7 [‡]	55.96	3.5	53.0	A	4	10-25	0.8	56.4				
2-2, 48	56.37	2.0	41.0	A				66.5				
2-2, 68 [‡]	56.57	1.7	37.6	A	5	10-28	1.5	68.9				
2-2, 100 [‡]	56.89	0.6	40.5	A	4	10-25	3.0	66.9				
2-2, 110	57.02	3.3	44.1	A				64.1				
2-2, 131	57.23	2.5	46.1	A				62.5				
2-3, 29	57.71	2.5	46.9	A				61.9				
2-3, 74 [‡]	58.16	1.1	47.3	A	3	10-25	2.8	61.5				
2-3, 86 [‡]	58.28	1.4	47.1	A	4	10-25	3.8	61.7				
2-3, 106 [‡]	58.48	0.9	38.5	A	4	5-20	7.5	68.3				
2-3, 113	58.56	4.4	57.4	A				52.0				
3-1, 3	63.55	2.3	44.7	A				63.7				
3-1, 29 [‡]	63.81	1.7	41.0	A	4	10-25	2.8	66.5				
3-1, 51 [‡]	64.03	0.9	38.9	A	4	10-25	2.9	68.0				
3-1, 97 [‡]	64.49	1.8	39.1	A	4	10-25	2.1	67.9				
3-1, 119 [‡]	64.71	0.7	38.3	A	4	10-25	4.3	68.5				
3-1, 132	64.84	2.7	40.5	A				66.9				
3-2, 14 [‡]	65.16	0.8	51.9	A	4	10-25	1.5	57.5				
3-2, 23	65.25	2.2	35.3	A				70.5				
3-2, 26	65.42	2.5	36.7	A				69.6				
597C-												
3-1, 18 [‡]	55.67	3.0	37.4	A	4	10-25	0.7	69.1				
3-1, 24	55.73	2.8	45.7	A				62.9				
3-1, 48 [‡]	55.97	0.6	32.3	A	4	10-25	5.6	72.5				
3-1, 78 [‡]	56.27	0.6	Unstable	A								
3-1, 104 [‡]	56.53	0.8	47.7	A	3	10-20	4.2	61.2				
3-1, 134	56.83	3.1	50.1	A				59.1				
3-2, 13 [‡]	57.12	0.9	Unstable	A								
3-2, 43	57.42	2.4	36.5	A				69.7				
3-2, 81 [‡]	57.80	1.1	45.4	A	4	10-25	2.8	63.1				
3-2, 123 [‡]	58.22	1.6	33.6	A	4	10-25	2.5	71.6				
3-2, 146 [‡]	58.45	2.6		A								
3-3, 5	58.57	2.7	60.1	A				49.0*				
3-3, 38 [‡]	58.90	2.5	32.4	A	4	10-25	0.4					
3-3, 52	59.04	2.5	31.2	A				73.2				
3-3, 71 [‡]	59.23	4.2	43.1	A	4	10-25	1.5	64.9				
4-1, 55 [‡]	65.07	1.9	Unstable	A								
4-1, 60	65.12	4.1	37.9	A				68.7				
4-1, 70 [‡]	65.22	0.6	-58.4 [†]	A	4	15-28	2.4	50.9				
4-1, 120	65.72	3.3	41.3	A				66.3				
4-2, 21	66.72	3.1	48.2	A				<u>60.8</u>	<u>1</u>	<u>62.8</u>	<u>5.5</u>	<u>39</u>
4-2, 55 [‡]	67.06	1.1	61.7	A	3	10-20	4.3	47.1				
4-2, 87 [‡]	67.38	2.3	-63.3 [†]	A	3	28-35	3.4	45.2				
4-2, 109 [‡]	67.60	1.8	Unstable	A								
4-2, 111	67.13	2.9	55.8	A				53.7				
4-3, 27	67.79	3.3	60.4	A				48.6				
4-3, 49 [‡]	68.01	3.7	Unstable	A								
4-3, 91	68.43	2.7	61.0	A				<u>47.9</u>	<u>2</u>	<u>48.5</u>	<u>3.2</u>	<u>5</u>
4-3, 139 [‡]	68.91	2.2	Unstable	A								
4-4, 23	69.25	2.7	44.9	A				63.5				
4-4, 62 [‡]	69.64	5.1	53.5	A	3	10-20	2.9	56.0				
4-4, 76	69.78	3.3	48.5	A				60.5				
4-4, 127 [‡]	70.29	2.0	Unstable	A								
4-5, 23 [‡]	70.75	2.6	Unstable	A								
4-5, 26	70.78	2.3	45.3	A				63.2				
4-5, 71	71.22	2.3	45.6	A				63.0				
4-5, 89 [‡]	71.41	1.0	Unstable	A								
4-5, 118 [‡]	71.70	2.2	Unstable	A								
4-6, 21	72.22	2.3	65.7	A				42.1*				
4-6, 42 [‡]	72.43	1.3	Unstable	A								
4-6, 73	72.75	2.0	43.0	A				65.0				

Table T4 (continued).

Core, section, interval (cm)	Depth (mbsf)	NRM (A/m)	Inc (°)	Demag	N	Steps	MAD (°)	Colatitude (°)	Group number	Mean colat	Std	N colat
4-6, 100 [‡]	73.01	2.2	53.0	A	4	10-25	1.5	56.4				
5-1, 9 [‡]	73.61	1.2	Unstable	A								
5-1, 62 [‡]	74.14	7.3	52.2	A	3	10-20	2.2	57.2				
5-1, 129	74.81	2.6	41.0	A				66.5				
5-1, 134 [‡]	74.86	1.2	41.2	A	3	10-20	3.0	66.4				
5-2, 63	75.64	4.0	46.1	A				<u>62.5</u>	<u>3</u>	<u>61.8</u>	<u>3.8</u>	<u>11</u>
6-1, 28 [‡]	82.80	2.3	Unstable	A								
6-1, 109	83.61	3.6	50.6	A				58.7				
6-1, 119 [‡]	83.71	4.6	56.4	A	3	10-20	0.4	53.0				
6-2, 12 [‡]	84.14	1.5	-34.6 [†]	A	3	10-20	1.8	71.0*				
6-2, 35 [‡]	84.37	1.3	47.4	A	4	10-25	4.5	61.5				
6-2, 49	84.51	2.3	46.5	A				62.2				
6-3, 62	86.14	2.9	49.3	A				59.8				
6-3, 55 [‡]	86.07	2.1	Unstable	A								
6-3, 78 [‡]	86.30	1.0	Unstable	A								
6-3, 105	86.57	0.7	49.2	A	4	25-35	2.1					
6-4, 19 [‡]	87.21	2.4	54.6	A	4	10-25	3.6	<u>54.9</u>	<u>4</u>	<u>58.3</u>	<u>3.7</u>	<u>7</u>
6-4, 53 [‡]	87.55	1.7	Unstable	A								
6-4, 74	87.76	3.0	37.8	A				68.8				
6-4, 116 [‡]	88.18	2.1	Unstable	A								
6-5, 38 [‡]	88.90	0.6	27.5	A	3	10-20	3.5	75.4				
6-5, 58	89.10	3.3	37.9	A				68.7				
6-5, 82 [‡]	89.34	2.3	Unstable	A								
7-1, 70 [‡]	92.22	1.8	31.0	A	4	15-28	2.2	<u>73.3</u>	<u>5</u>	<u>71.6</u>	<u>3.3</u>	<u>4</u>
7-1, 128 [‡]	92.80	5.8	48.1	A	4	10-25	1.6	60.9				
7-1, 115	92.67	3.1	50.2	A				59.0				
7-2, 7 [‡]	93.08	2.8	Unstable	A								
7-2, 16	93.17	3.3	45.6	A				63.0				
7-2, 66 [‡]	93.67	6.7	49.8	A	4	15-20	2.4	59.4				
7-2, 117	94.18	3.7	50.6	A				58.7				
7-2, 123 [‡]	94.24	3.9	47.4	A	4	10-25	0.5	61.5				
7-3, 10 [‡]	94.61	4.3	55.2	A	4	10-25	0.7	54.3				
7-4, 17 [‡]	96.19	5.2	58.9	A	4	10-25	2.5	50.3				
7-4, 18	96.20	3.0	54.0	A				55.5				
7-4, 87	96.89	4.4	50.2	A				59.0				
7-4, 91 [‡]	96.93	6.7	-49.9 [†]	A	4	28-35	2.2	59.3				
7-4, 111	97.13	2.8	56.0	A				53.5				
7-4, 137	97.39	1.9	-41.1 [†]	A				66.4				
7-4, 141 [‡]	97.43	2.3	-65.6 [†]	A	4	5-20	1.2	42.2*				
7-5, 70	98.22	2.2	-76.7 [†]	A				<u>25.3*</u>	<u>6</u>	<u>58.5</u>	<u>4.3</u>	<u>13</u>
8-1, 9	100.60	3.2	41.9	A				65.8				
8-1, 25 [‡]	100.76	1.8	39.6	A	4	10-25	2.0	67.5				
8-1, 94	101.46	3.2	41.0	A				66.5				
8-1, 103 [‡]	101.54	3.7	40.4	A	4	15-28	1.2	66.9				
8-2, 41 [‡]	102.42	3.5	41.0	A	4	10-25	1.9	66.5				
8-2, 50	102.51	2.8	39.1	A				67.9				
8-2, 66 [‡]	102.67	2.2	41.3	A	3	10-20	2.3	66.3				
8-2, 137 [‡]	103.38	2.7	46.1	A	4	15-28	1.5	62.5				
8-3, 5	103.57	2.5	36.5	A				69.7				
8-3, 44 [‡]	103.96	1.5	Unstable	A								
8-3, 130	104.82	2.5	22.1	A				78.5*				
8-3, 138 [‡]	104.90	2.4	30.8	A	5	10-28	2.6	73.4				
8-4, 70 [‡]	105.72	1.8	31.7	A	4	10-25	4.9	72.8				
8-4, 102	106.04	2.6	40.2	A				67.1				
8-4, 103 [‡]	106.05	2.9	43.5	A	4	15-28	1.7	64.6				
8-4, 137 [‡]	106.39	1.0	33.1	A	3	20-28	2.3	71.9				
8-5, 49	107.01	3.9	34.8	A	4	10-25	0.3	70.8				
8-5, 60	107.12	2.7	37.0	A				69.4				
8-5, 88 [‡]	107.40	2.5	Unstable	A								
8-6, 30 [‡]	108.32	1.3	32.1	A	4	10-25	2.7	72.6				
8-6, 56	108.58	3.3	40.9	A				66.6				
8-6, 92 [‡]	108.94	1.2	-22.7 [†]	A	3	20-28	0.7	78.2*				
8-6, 135 [‡]	109.37	2.7	37.2	A	4	10-25	3.7	69.2				
8-7, 7 [‡]	109.57	1.4	41.6	A	3	15-25	1.9	66.1				
8-7, 9	109.59	2.9	44.0	A				64.2				
8-7, 86 [‡]	110.36	2.0	28.9	A	4	10-25	6.3	74.6				
9-1, 9	109.59	3.8	36.5	A				69.7				
9-1, 76 [‡]	110.27	0.8	Unstable	A								
9-1, 139	110.90	2.2	34.5	A	4	15-28	1.7					

Table T4 (continued).

Core, section, interval (cm)	Depth (mbsf)	NRM (A/m)	Inc (°)	Demag	N	Steps	MAD (°)	Colatitude (°)	Group number	Mean colat	Std	N colat
9-1, 141‡	110.92	1.4	Unstable	A								
9-1, 142	110.93	3.2	38.9	A				68.0				
9-2, 15‡	111.17	2.8	60.8	A	4	20-35	1.4	48.2*				
9-2, 60‡	111.62	3.3	-46.6†	A	5	30-45	0.4	62.1				
9-2, 70	111.72	3.4	41.6	A				66.1				
9-3, 82‡	113.33	1.1	-60.6†	A	7	28-45	5.7	48.4*				
9-3, 88	113.39	2.9	47.3	A				61.5				
9-3, 140‡	113.91	0.9	-51.3†	A	4	20-30	5.1	58.0				
9-4, 64‡	114.66	0.6	Unstable	A								
9-4, 103	115.05	3.1	41.9	A				65.8				
9-4, 104‡	115.06	4.6	33.9	A	4	20-30	6.2	<u>71.4</u>	Z	<u>67.5</u>	<u>3.8</u>	<u>30</u>
10-1, 74‡	119.26	6.5	43.4	A	4	15-25	2.0	64.7				
10-1, 112	119.64	2.9	40.1	A				67.2				
10-1, 128‡	119.80	2.9	37.5	A	4	10-25	2.2	69.0				
10-2, 39‡	120.41	2.5	44.5	A	4	10-25	0.6	63.8				
10-2, 86‡	120.88	1.9	52.9	A	4	10-25	3.3	56.5				
10-2, 104	121.06	1.9	43.6	A				64.5				
10-3, 33‡	121.85	0.9	Unstable	A								
10-3, 72‡	122.24	2.1	42.7	A	4	20-35	1.1	65.2				
10-3, 94	122.46	2.0	43.9	A				64.3				
10-3, 115‡	122.67	2.2	31.8	A	4	10-25	4.3	72.8				
10-4, 46‡	123.48	1.0	39.6	A	4	10-25	2.9	67.5				
10-4, 91	123.93	1.5	52.6	A				56.8				
10-4, 133‡	124.35	1.1	32.8	A	3	10-20	4.6	72.1				
10-5, 52‡	125.02	1.0	Unstable	A								
10-5, 84	125.36	1.6	46.4	A				62.3				
10-5, 112‡	125.62	2.1	-49.5†	A	4	15-28	0.2	59.7				
10-6, 19‡	126.21	0.5	46.1	A	4	20-30	2.6	62.5				
10-6, 36	126.38	1.7	40.5	A				66.9				
10-6, 103‡	127.05	0.9	44.8	A	4	20-30	1.6	63.6				
10-7, 30‡	127.31	1.4	45.5	A	4	15-28	1.7	63.0				
10-7, 42	127.93	1.6	42.2	A				65.6				
10-7, 84	127.85	1.2	21.0	A	4	15-28	1.0	79.1*				
11-1, 32‡	127.84	0.7	63.8	A	4	20-30	0.6	44.5*				
11-1, 79	128.31	1.6	47.1	A				61.7				
11-1, 116‡	128.68	0.4	44.7	A	4	15-28	1.2	63.7				
11-2, 46‡	129.48	0.7	Unstable	A								
11-2, 103	130.05	1.6	43.8	A				64.4				
11-2, 138‡	130.40	0.7	48.1	A	4	25-40	0.4	60.9				
11-3, 13	130.64	1.7	45.6	A				63.0				
11-3, 47‡	130.98	1.8	41.6	A	4	10-25	0.9	66.1				
11-3, 93‡	131.44	1.2	40.4	A	4	15-28	0.9	66.9				
11-4, 25‡	132.26	0.9	23.2	A	4	10-25	3.3	77.9*				
11-4, 39‡	132.40	1.4	-45.2†	A	4	25-32	1.2	63.3				
11-4, 50‡	132.51	1.6	47.0	A	4	10-25	1.1	61.8				
11-4, 62	132.63	1.7	42.9	A				65.1				
11-4, 66‡	132.67	1.6	32.2	A	4	10-25	0.5	<u>72.5</u>	8	<u>64.6</u>	<u>3.9</u>	<u>30</u>

Notes: NRM = natural remanent magnetization. Inc = inclination of characteristic remanent magnetization determined by principal component analysis. Demag = demagnetization. A = alternating field. N = number of measurements used for principal component analysis. Steps = demagnetization steps used for principal component analysis. MAD = maximum angle of deviation (Kirshvink, 1980). Mean colat = group mean colatitude. Std = standard deviation of group mean colatitude. N colat = number of colatitudes used to calculate group mean. * = datum not used in average colatitude calculations. Group averages are shown at the far right; underscores show the division of groups. † = Sample assumed to be inverted. ‡ = Sample measured in this study.

Table T5. Paleomagnetic data for igneous samples, Sites 800, 803, and 865. (See table notes. Continued on next page.)

Core, section, interval (cm)	Depth (mbsf)	NRM (A/m)	Inc (°)	Demag	N	Steps	MAD (°)	Colatitude (°)	Group number	Mean colat	Std	N colat
800- (Core 57 assumed normal polarity; Cores 58 and 60 assumed reversed)												
57-1, 30	498.30	0.2	15.0 [†]	A/T	2	15-150	1.7	97.6				
57-2, 16	499.66	0.4	-22.7	A/T	4	200-375	3.8	101.8				
57-2, 24	499.74	0.5	-35.7	A/T	4	250-350	6.1	109.8				
57-2, 40	499.90	0.6	-20.2	A	4	20-35	3.8	100.4				
57-2, 60	500.10	0.6	-15.3	A/T	2	15-150	0.8	<u>97.8</u>	<u>1</u>	<u>101.5</u>	<u>5.0</u>	<u>5</u>
58-1, 6	507.26	1.2	Unstable	A/T								
58-1, 9	507.29	0.9	Unstable	A/T								
58-1, 25	507.45	1.0	Unstable	A								
58-1, 74	507.94	2.0	Unstable	A/T								
58-1, 118	508.38	1.6	Unstable	A								
58-2, 40	509.10	2.1	Unstable	A/T								
58-2, 79	509.49	1.5	Unstable	A/T								
58-2, 117	509.87	1.2	Unstable	A								
58-3, 22	510.42	9.8	42.4	A/T	3	200-300	14.1	114.5				
58-3, 52	510.72	1.2	Unstable	A								
60-1, 10	526.00	1.2	26.4	A	4	10-25	8.4	103.9				
60-1, 37	526.27	2.3	15.2	A/T	3	15-200	7.5	97.7				
60-1, 93	526.83	1.4	39.5	A/T	3	150-250	2.6	112.4				
61-1, 4	535.34	1.9	39.7	A	4	15-30	6.0	<u>112.5</u>	<u>2</u>	<u>108.2</u>	<u>7.2</u>	<u>5</u>
803-												
69-1, 13	631.53	1.1	-50.5	A	7	22-38	0.7	121.2				
69-1, 24	631.64	6.5	-49.6	A	5	20-40	1.5	120.4				
69-1, 89	632.29	1.8	-46.3	A	5	25-45	1.3	117.6				
69-1, 105	632.45	3.3	-43.4	A	4	25-40	1.3	115.3				
69-2, 17	633.07	1.6	-42.7	A	4	15-25	0.7	114.8				
69-2, 111	634.01	2.6	-43.6	A	5	22-32	1.1	115.5				
69-2, 133	634.23	1.6	46.0 [†]	A	3	10-20	0.2	117.4				
69-3, 20	634.60	1.6	-52.4	A	6	22-35	0.7	123.0				
69-3, 102	635.42	1.6	-47.4	A	5	20-40	1.0	118.5				
70-1, 140	642.50	1.7	-46.4	A	4	25-40	1.6	117.7				
70-2, 2	642.62	1.6	-48.2	A	6	22-35	1.4	119.2				
70-2, 52	643.12	3.2	-55.1	A	6	22-35	0.9	125.6				
70-3, 37	644.47	3.6	-41.8	A	6	22-35	1.9	<u>114.1</u>	<u>1</u>	<u>118.5</u>	<u>3.4</u>	<u>13</u>
71-1, 35	651.15	2.0	-37.6	A	5	15-28	0.9	111.1				
71-1, 70	651.50	7.7	-33.0	A	5	15-28	0.8	108.0				
71-1, 139	652.19	1.8	-43.4	A	3	15-25	1.0	115.3				
71-2, 66	652.96	4.7	-36.7	A	5	15-28	1.0	110.4				
71-2, 139	653.69	2.3	-41.0	A	5	25-35	1.0	113.5				
71-3, 42	654.22	3.6	-44.3	A	4	15-25	1.0	116.0				
71-3, 53	654.33	3.2	-38.7	A	5	20-28	1.0	<u>111.8</u>	<u>2</u>	<u>112.3</u>	<u>2.8</u>	<u>7</u>
865-												
90-5, 129	839.09	1.2	-20.1	A	6	25-50	0.4	100.4				
90-6, 8	839.38	5.4	-29.2	A	7	20-50	0.8	105.6				
90-6, 47	839.77	5.4	-18.2	A	7	20-50	0.6	<u>99.3</u>	<u>1</u>	<u>101.8</u>	<u>3.4</u>	<u>3</u>
91-1, 120	842.30	1.4	-38.7	A	4	15-30	0.5	111.8				
91-2, 27	842.87	6.0	-28.9	A	5	15-35	0.9	105.4				
91-2, 127	843.87	5.6	-36.3	A	6	20-45	2.0	110.2				
91-3, 9	844.19	1.5	-38.8	A	4	15-30	0.6	111.9				
91-4, 107	846.67	1.2	-30.6	A	7	20-50	0.3	106.5				
92-4, 55	852.25	3.3	-30.2	A	7	20-50	0.4	<u>106.2</u>	<u>2</u>	<u>108.7</u>	<u>3.0</u>	<u>6</u>
92-5, 18	853.38	3.7	-20.6	A	5	15-35	0.4	100.6				
92-5, 26	853.46	3.0	-19.0	A	5	15-35	1.3	99.8				
93-2, 3	854.93	3.4	-21.4	A	6	25-45	0.4	101.1				
93-2, 120	856.10	3.8	-25.5	A	6	25-50	0.9	103.4				
93-3, 26	856.66	1.8	-20.8	A	5	20-40	2.2	100.8				
93-3, 75	857.15	3.0	-24.2	A	6	15-40	2.2	102.7				
94-1, 77	863.87	8.7	-31.9	A	5	20-40	1.1	107.3				
94-1, 136	864.46	3.8	-30.4	A	5	20-40	0.8	106.4				
94-2, 44	865.04	5.6	-28.3	A	5	20-40	0.6	105.1				
94-2, 55	865.15	3.0	-27.1	A	5	20-40	1.4	104.4				
94-4, 57	868.17	1.9	-30.3	A	5	20-40	0.6	106.3				
94-4, 63	868.23	8.1	-29.5	A	5	20-40	0.5	105.8				
94-4, 119	868.79	9.5	-29.0	A	5	20-40	0.3	<u>105.5</u>	<u>3</u>	<u>103.8</u>	<u>2.6</u>	<u>13</u>

Notes: NRM = natural remanent magnetization. Inc = inclination of characteristic remanent magnetization determined by principal component analysis. Demag = demagnetization. A = alternating field, T = thermal. *N* = number of measurements used for principal component analysis. Steps = demagnetization steps used for principal component analysis. MAD = maximum angle of deviation (Kirshvink, 1980). Mean colat = group mean colatitude. Std = standard deviation of group mean colatitude. *N* colat = number of colatitudes used to calculate group mean. Group averages are shown at the far right; underscores show the division of groups. † = sample assumed to be inverted.